FULL PAPER

Dalton
www.rsc.org/dalton

Dicopper(I,I) and delocalized mixed-valent dicopper(I,II) complexes of a sterically hindered carboxylate ligand

John R. Hagadorn, Theresa I. Zahn, Lawrence Que, Jr.* and William B. Tolman*
Department of Chemistry, Center for Metals in Biocatalysis, University of Minnesota, 207 Pleasant St. SE, Minneapolis, MN 55455, USA. E-mail: que@chem.umn.edu. E-mail: tolman@chem.umn.edu; Fax: 612 624 7029; Tel: 612 625 0389, 4061

Received 29th January 2003, Accepted 17th March 2003
First published as an Advance Article on the web 28th March 2003

Admixture of the lithium salt of the bulky ligand 2,6-dimesitylbenzoate $[ArCO_2]^-$ with $[Cu(CH_3CN)_4]O_3SCF_3$ yielded the dicopper(I,I) complex $[(ArCO_2)_2Cu_2(THF)_2)]$ (**1**), which upon oxidation with AgX (X = SbF_6^- or ClO_4^-) in THF afforded the mixed-valent complexes $[(ArCO_2)_2Cu_2(THF)_2]SbF_6$ (**2**) and $[(ArCO_2)_2Cu_2(THF)_3]ClO_4$ (**3**), respectively. Fully delocalized mixed-valent ($Cu^{1.5}Cu^{1.5}$) formulations for **2** and **3** were determined on the basis of X-ray crystallography and UV-vis, resonance Raman, ^1H NMR, and EPR spectroscopy. Notably, solvent dependent UV-vis spectra suggest that THF and/or counter ion coordination influence the intermetal bonding interactions in the mixed-valent cores.

Introduction

Since the discovery[1] of the novel mixed-valent bis(thiolato)-dicopper "Cu_A" electron transfer biosite in which an unpaired electron is fully delocalized between the two metal ions (*i.e.*, class III mixed valent behavior),[2] interest has focused on understanding its unique structural, spectroscopic, and functional properties.[3] As a means toward these ends, $Cu^{1.5}Cu^{1.5}$ compounds have been targeted for synthesis and in-depth characterization.[4–10] A key challenge in designing such species is enforcing full delocalization in a mixed-valent dicopper complex, which more typically adopts an unsymmetric structure with the unpaired electron localized to a significant extent on one site (class I or II).[11] Most of the ligands used successfully so far to access fully delocalized mixed valent complexes sequester the copper ions in a symmetrical environment that also inhibits intermolecular reactions (*e.g.*, disproportionation). For example, class III $Cu^{1.5}Cu^{1.5}$ complexes were prepared using the XDK ligand system (Fig. 1(a)),[7] in which the effects of steric hindrance and preorganization of the ligating carboxylate groups combine to stabilize the mixed valent core (as well as other biologically relevant dimetal species)[12] sufficiently for structural and spectroscopic characterization. In a complementary approach, sterically hindered benzoate ligands (Fig. 1(b)) have been used in order to prepare coordinatively unsaturated and reactive iron complexes that model key aspects of metalloprotein active sites.[13] A dicopper(II,II) complex bridged by a bulky benzoate was reported recently.[14] Here, we show that such ligands also may be used to construct dicopper(I,I) complexes and class III mixed valent species derived therefrom. Although similar to other delocalized mixed-valent dicopper complexes with respect to their structures and EPR and resonance Raman spectral properties, the examples of such compounds we have prepared exhibit interesting ^1H NMR spectral properties and solvent-dependent electronic absorption spectral features that implicate subtle effects of solvent and/or counter ion coordination on the Cu–Cu interaction.

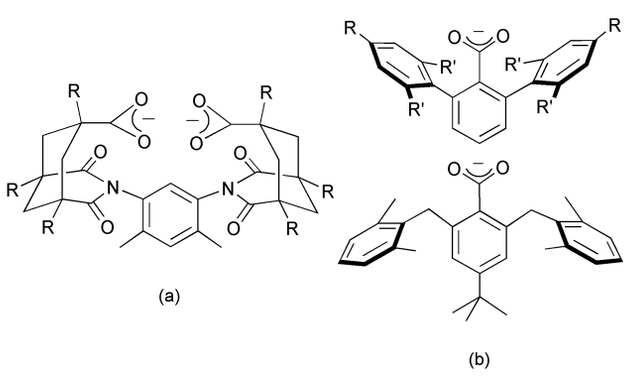

Fig. 1 (a) XDK ligand system (R = Me, Pr, Bn). (b) Sterically hindered carboxylates (R = Me, R′ = H or Me).

Results and discussion

Syntheses and structures

Treatment of $[ArCO_2]Li(Et_2O)_{0.5}(CH_3CN)_{0.5}$ with 1 equiv. $[Cu(CH_3CN)_4]O_3SCF_3$ yielded $[(ArCO_2)_2Cu_2(THF)_2)]$ (**1**) as colorless crystals in moderate yield (Scheme 1). As shown by X-ray crystallography (Fig. 2, Table 1), **1** adopts a discrete molecular structure that features inversion symmetry, a short Cu–Cu separation of 2.524(1) Å, and three-coordinate Cu(I) ions in a T-shaped geometry. The overall structure contrasts with the oligo- or poly-meric topologies typical for Cu(I) complexes of simple carboxylates (*e.g.* acetate or benzoate),[15] but is similar to that of a class of dicopper(I,I) compounds prepared using XDK derivatives.[16] Thus, higher aggregate formation is effectively inhibited by the bulk of the $ArCO_2^-$ ligand, albeit through steric influences that differ from those factors that control complex nuclearity and structure in the preorganized XDK system. The high symmetry of the solid state structure of

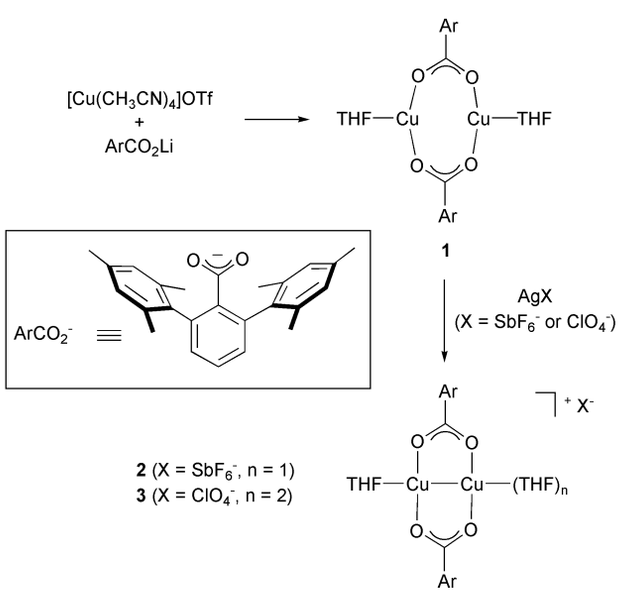

Scheme 1 Synthesis of complexes.

DOI: 10.1039/b301154b

Table 1 Selected bond distances (Å) and angles (°) for the X-ray structures of **1** and **3**[a]

1			
Cu1–Cu1A	2.524(1)	Cu1–O1	1.919(3)
Cu1–Cu1A	2.524(1)	Cu1–O2A	1.920(3)
Cu1–O3	2.247(3)		
O1–Cu1–O3	94.0(1)	O1–Cu1–O2A	170.3(1)
O3–Cu1–O2A	95.7(1)		
3			
Cu1–Cu2	2.3947(8)	Cu1–O6	2.146(4)
Cu1–O1	1.901(3)	Cu2–O2	1.882(3)
Cu1–O3	1.894(3)	Cu2–O4	1.881(3)
Cu1–O5	2.055(3)	Cu2–O7	2.022(4)
Cu2–O8	2.501(4)		
O3–Cu1–O1	164.1(2)	O3–Cu1–O5	92.4(2)
O1–Cu1–O5	89.5(1)	O3–Cu1–O6	100.4(2)
O1–Cu1–O6	95.3(2)	O5–Cu1–O6	92.4(2)
O4–Cu2–O2	167.2(2)	O4–Cu2–O7	91.6(2)
O2–Cu2–O7	93.6(2)		

[a] Estimated standard deviations are indicated in parentheses. Symmetry transformations used to generate equivalent atoms for **1** are $-x + 1$, $-y + 2$, $-z + 1$.

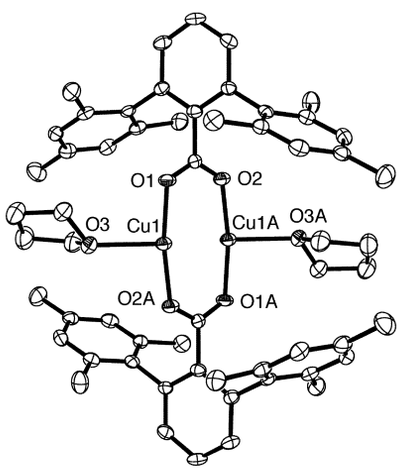

Fig. 2 Representation of the X-ray crystal structure of **1**, with all non-hydrogen atoms shown as 50% ellipsoids.

1 is retained in solution, as evinced by the single set of peaks for the carboxylate ligand and coordinated THF in its ^{1}H NMR spectrum.

Dropwise addition of THF solutions of AgX (1 equiv., X = SbF_6^- or ClO_4^-) to a colorless THF solution of **1** immediately yielded air-sensitive violet solutions and a dark precipitate (presumably, Ag^0) (Scheme 1). After filtration, purple crystalline products were formed by the addition of pentane and cooling to −30 °C. The products were identified as $[(ArCO_2)_2Cu_2(THF)_2]SbF_6$ (**2**) and $[(ArCO_2)_2Cu_2(THF)_3]ClO_4$ (**3**) as described below. † Upon exposure to vacuum, the crystals of the SbF_6^- salt became gray, and loss of coordinated THF was confirmed by elemental analysis. Interestingly, exposure of the gray solid to THF vapor resulted in conversion back to purple material, a process that may be repeated many times without apparent decomposition. Crystals of the ClO_4^- salt **3** suitable for an X-ray diffraction study were grown from a THF-pentane mixture (Fig. 3). The structure shows a dicopper core comprising Cu ions supported by a pair of μ-1,3-carboxylates and THF solvate molecules. Both Cu sites are square pyramidal, with the axial positions occupied by a weakly bonded ClO_4^- (Cu2–O8 2.501(4) Å) or a THF molecule (Cu1–O6 2.146(4) Å). The Cu–Cu distance (2.3947(8) Å) is significantly shorter than that of **1** (by >0.12 Å) and is comparable to the shortest value reported for a delocalized mixed valence dicopper complex (2.3876(12) Å).[6] Since Cu–Cu bonding has been implicated for other mixed-valence species with similar, or even slightly longer metal–metal distances, an analogous intermetal bonding interaction is indicated. This conclusion is supported by spectroscopic data for both **2** and **3**, as described below. A preliminary X-ray crystal structure was acquired for **2**, but a full structure solution was not possible due to the quality of the data. ‡ Nonetheless, a molecular topology analogous to that of **3** was discernible, the only notable difference being the absence of an axial THF solvate molecule on one Cu ion and the presence of SbF_6^- weakly bonding to the axial position of the other.

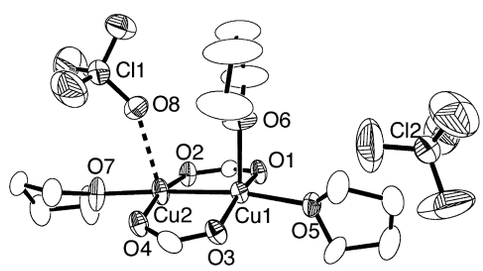

Fig. 3 Representations of the X-ray structure of **3**, with all non-hydrogen atoms shown as 50% ellipsoids and the carboxylate substituents omitted for clarity.

Spectroscopic features

The EPR spectra of **2** and **3** exhibit a rhombic signal with extensive hyperfine features, including a clearly discernible seven-line pattern at low field due to coupling to two $I = 3/2$ Cu ions (shown for **2** in Fig. 4, bottom; 1 : 1 THF–toluene, X-band, 2 K). The following g values and hyperfine parameters were determined *via* spectral simulation (Fig. 4, top): $g_1 = 2.027$, $g_2 = 2.159$, $g_3 = 2.309$, $A^{Cu}{}_1 = 22.5$ G, $A^{Cu}{}_2 = 63.0$ G, $A^{Cu}{}_3 = 132.9$ G. The signals confirm class III mixed valence formulations for **2** and **3**, and are similar to those exhibited for other reported examples of such species.[4,6–8]

The ^{1}H NMR spectrum of crystals of **2** in $CDCl_3$ (Fig. 5) reveals six broadened and slightly shifted features in the

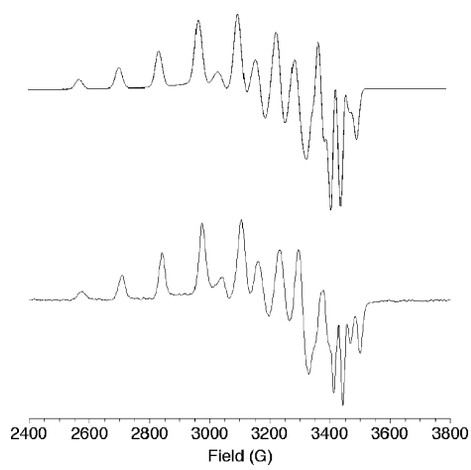

Fig. 4 X-Band EPR spectrum (bottom) and simulation (top) of **2** in 1 : 1 THF–toluene, 2 K.

† Cyclic voltammograms of **2** measured in THF (0.5 M Bu_4NPF_6, Pt electrode) showed an irreversible oxidation at +0.076 V *vs.* Fc–Fc^+.

‡ Unit cell information: $C_{62}H_{74}ClCu_2O_{11}$, $M = 1157.74$, orthorhombic, *Pbcn*, $a = 19.007(1)$ Å, $b = 24.185(1)$ Å, $c = 25.356(2)$ Å, $V = 11656(1)$ Å^3, $Z = 8$.

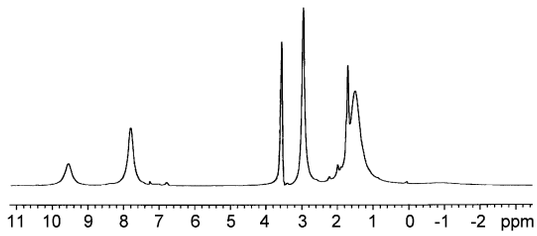

Fig. 5 ^{1}H NMR spectrum of **2** ($CDCl_3$, 300 MHz, room temp.).

0–10 ppm range. The simplicity of the spectrum, comparable to that of its precursor **1**, indicates that the equivalence of the carboxylate ligands is maintained upon one-electron oxidation, consistent with the valence delocalized description of the complex. Given the relative sharpness of the NMR features, the valence delocalized dicopper(I,II) center in **2** has an electronic relaxation time (T_{1e}) much shorter than that typical of a mononuclear Cu(II) center (~10^{-9} s), as noted previously for the biological Cu_A site.[17,18] Assignment of the six observed signals can be made upon consideration of relative peak areas, linewidths, and metal–proton distances (δ (ppm): 9.5 (2H, *m*-H); 7.8 (4H, THF β-H); 3.6 (4H, *m*′-H); 2.9 (6H, *p*′-Me); 1.7 (1H, *p*-H); 1.5 (12H, *o*′-Me)). Only the α-THF protons are not observed, which is not surprising considering their proximity to the paramagnetic metal center.

As noted above, the color of solid **2** is affected by the absence or presence of THF; crystalline **2** is gray under vacuum, purple in the presence of excess THF vapor, and red when crystallized from toluene (two THF molecules coordinated). In addition, UV-vis spectra of **2** and **3** in solution are influenced by the nature of the solvent (*cf.* data for **2** shown in Fig. 6). Solutions of **2** in THF are purple, with intense bands at λ_{max} = 379 (ε = 2400 M^{-1} cm^{-1}), 534 (1300) and 941 (1000) nm (Fig. 6, solid line). These bands shift appreciably for **2** dissolved in toluene (red, dot–dash line) or CH_2Cl_2 (green–brown, dotted line), with the low energy feature changing the most (941 ⟶ 788 ⟶ 736 nm). For **3**, the low energy absorption shifts from 911 nm (THF) to 753 nm (CH_2Cl_2).

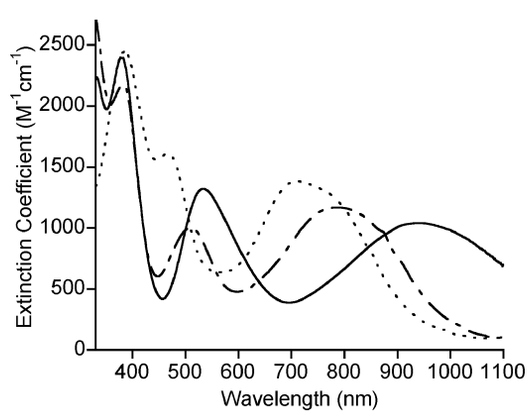

Fig. 6 Electronic absorption spectra of **2** at 25 °C in THF (solid), toluene (dot–dash), and CH_2Cl_2 (dotted).

Conversion of the spectral features for **2** in CH_2Cl_2 upon titration with THF is shown in Fig. 7. The dependence of the spectrum on the concentration of THF indicates a complex equilibrium in which the initial molecule (0% THF) converts to a different species (30% THF), with no isosbestic points apparent when all spectra are overlayed. Upon closer inspection, there is an isosbestic point at ~650 nm at low THF concentrations (<3%) and at ~600 nm at higher concentrations (4–30%). The involvement of an intermediate(s) in the conversion of the species in CH_2Cl_2 to the one in THF is implicated by these data, but the nature of this intermediate(s) is not known at present.

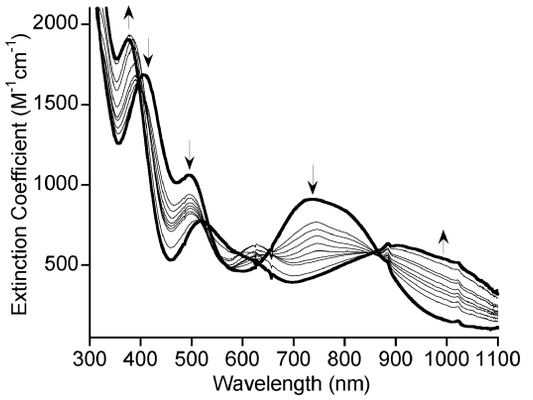

Fig. 7 Electronic absorption spectra acquired during the titration of **2** in CH_2Cl_2 with THF (up to 30% v/v).

The combined observations for solid **2** and for **2** and **3** in solution suggest that THF coordination and/or solvent polarity variation dramatically influence the absorption spectral features of these mixed valence complexes. The large solvent dependence of the λ_{max} of the low energy feature is most significant, since this feature is probably due to a $\Psi \longrightarrow \Psi^*$ transition of the mixed valence system. By analogy to previous studies of class III mixed valence dicopper compounds that feature short intermetal separations (<2.5 Å),[3,4,6–8] substantial metal–metal bonding/antibonding character for the wave functions involved in this transition is likely for **2** and **3**. Thus, it may be concluded that the $Cu^{1.5}Cu^{1.5}$ bonding interactions in **2** and **3** are perturbed by binding of THF molecules and/or altering counter ion coordination through solvent polarity changes. To our knowledge, these solvent effects are unique in mixed valence dicopper systems, although related influences of axial solvent coordination on metal–metal bonding interactions have been reported recently for $Rh_2(O_2CR)_4$ paddlewheel complexes.[19]

The apparent solvent dependent variation of the Cu–Cu interaction in **2** was further investigated through EPR and resonance Raman spectroscopy experiments, but with mixed results. Thus, while solutions of **2** in THF–toluene or CH_2Cl_2–toluene mixtures were purple and green–brown, respectively, at room temperature, both were violet when frozen, and EPR spectra acquired at 15 K for both samples were identical. In another attempt to probe the metal–metal interaction in **2**, we obtained a resonance Raman spectrum of a frozen THF solution using 514.5 nm laser excitation (Fig. 8). A strongly enhanced band appears at 244 cm^{-1}, with weaker features at 182, 482 and 738 cm^{-1}. The positions of the latter two bands are close to values predicted for overtones of the primary 244 cm^{-1} peak (488 and 732 cm^{-1}). We tentatively assign the primary band as a vibration with significant Cu–Cu stretching character, by analogy to assignments of similar bands reported in the range 241–289 cm^{-1} for $Cu^{1.5}Cu^{1.5}$ cryptate complexes.[20,21] While a previous study demonstrated extreme sensitivity of this Cu–Cu

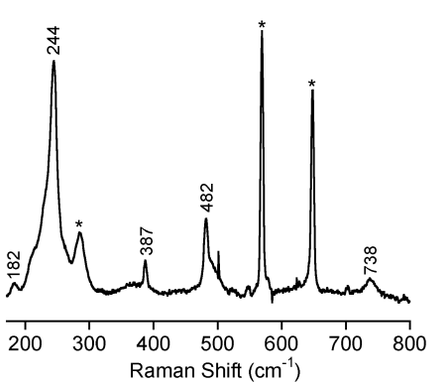

Fig. 8 Resonance Raman spectrum of **2** in THF (77 K, λ_{ex} = 514.5 nm). Asterisks (*) label peaks arising from the solvent.

mode to solvent (leading to the conclusion that ligand conformational isomerism underlies the mode shifts),[21] spectra of **2** in frozen CH_2Cl_2 or toluene were the same as that in THF. Attempts to obtain spectra at room temperature have not yet been successful. Thus, while we have been able to identify a Cu–Cu vibrational mode by Raman spectroscopy, we have been unable to corroborate by this method the conclusion derived from UV-vis data that the Cu–Cu interaction is perturbed by changing the solvent.

Conclusions

We have described a dicopper(I) complex of a carboxylate ligand, employing self assembly methods and taking advantage of its steric bulk to prevent oligomerization. One-electron oxidation affords a dicopper(I,II) complex, the spectroscopic properties of which clearly demonstrate Class III mixed-valent behavior analogous to that found for other dicopper complexes with Cu–Cu distances of less than 2.5 Å. The unusually large solvent dependence we have observed in the absorption features of its electronic spectrum suggests that the metal–metal interactions that give rise to the valence delocalized behavior can significantly be perturbed by solvent and/or counter ion binding. Unfortunately, further study of this phenomenon with spectroscopic techniques that can provide more detailed molecular insight such as ESR and Raman may be precluded by the apparent conversion of all forms into spectroscopically indistinguishable species below 77 K.

Experimental

General

Standard Schlenk-line and glovebox techniques were used for the handling of all compounds. Tetrahydrofuran (THF), pentane and toluene were distilled from Na/benzophenone ketyl, and CH_3CN, hexamethyldisiloxane (HMDSO) and CH_2Cl_2 were distilled from CaH_2 under nitrogen. $CDCl_3$ was vacuum transferred from CaH_2. Chemical shifts for ^{1}H NMR spectra are given relative to residual protium in the deuterated solvents. X-Band EPR spectra were recorded using a Bruker E-500 spectrophotometer with the temperature (2–20 K) regulated by an Oxford Instruments EPR-10 liquid-helium cryostat. Spectra were recorded with a modulation amplitude of 10 G and a modulation frequency of 100 kHz. Spin quantification was performed by comparison to a 1 mM sample of [L^{HAmMe}-CuCl]ClO_4.[22] Resonance Raman spectra were collected on an Acton 506 spectrometer using a Princeton Instruments LN/CCD-1100-PB/UVAR detector and ST-1385 controller interfaced with Winspec software. A Spectra-Physics 2030-15 argon ion laser was used to give the excitation wavelength at 457.9 and 514.5 nm; laser power was *ca.* 50 mW at the sample. The spectra were obtained at *ca.* 77 K using a 135° backscattering geometry; solutions of samples were frozen onto a gold-plated copper cold finger in thermal contact with a Dewar flask containing liquid nitrogen. Spectra in pixel units were converted to frequency units by a quadratic fit of pixels to several peaks in the known spectrum of indene. Spectra were generally recorded with slits set for a band-pass of 4 cm^{-1}. Elemental analyses were determined by Atlantic Microlab, Inc. Single crystal X-ray diffraction data were collected using a Siemens SMART diffractometer. The compounds $[Cu(CH_3CN)_4]O_3SCF_3$[23] and $[ArCO_2]Li(Et_2O)_{0.5}(CH_3CN)_{0.5}$[24] were prepared according to reported procedures. All other chemicals were purchased from Aldrich and used as received.

Preparation of $[(ArCO_2)_2Cu_2(THF)_2)]$ (1)

Toluene (40 mL) and CH_3CN (10 mL) were added to a flask charged with solid $[Cu(CH_3CN)_4]O_3SCF_3$ (0.638 g, 1.69 mmol) and $[ArCO_2]Li(Et_2O)_{0.5}(CH_3CN)_{0.5}$ (0.723 g, 1.69 mmol), forming a colorless suspension. After ca. 20 h, CH_2Cl_2 (80 mL) was added and the mixture was filtered. The solvent was removed from the filtrate under vacuum and the residue was crystallized from a mixture of THF (25 mL) and HMDSO (25 mL) to yield the product as colorless crystals (0.250 g, 32%). ^{1}H NMR ($CDCl_3$, 300 MHz): δ 7.37 (t, J = 7.8 Hz, 1H, p-C_6H_3), 7.00 (d, J = 7.8 Hz, 2H, m-C_6H_3), 6.85 (s, 4H, m-Mes), 3.73 (m, 4H, THF), 2.33 (s, 6H, p-CH_3), 1.92 (s, 12H, o-CH_3), 1.85 (m, 4H, THF). Anal. Calc. for $C_{58}H_{66}O_6Cu_2$: C, 70.64, H, 6.75. Found: C, 71.14; H, 6.84%.

Preparation of $[(ArCO_2)_2Cu_2(THF)_2)]SbF_6$ (2)

To a solution of **1** (0.200 g, 0.216 mmol) in THF (10 mL) was added dropwise a solution of $AgSbF_6$ (0.074 g, 0.216 mmol) in THF (4 mL), forming a deep purple solution. The reaction mixture was filtered and concentrated to 5 mL. Upon addition of pentane (12 mL) crystals started to form, and crystallization was continued by allowing the mixture to stand for *ca.* 24 h at −30 °C. The deep purple crystals were collected, washed with pentane and dried under reduced pressure, after which the purple crystals became gray (0.147 g, 56%). Crystallization from toluene at −20 °C gave red crystals with two toluene solvate molecules that were suitable for X-ray diffraction studies. Addition of CH_3CN to a solution of **2** in THF resulted in the formation of a precipitate and a blue solution, interpreted as the disproportionation of the compound to Cu(0) and Cu(II). ^{1}H NMR (D_8-THF, 300 MHz): δ 9.58 ($\Delta w_{1/2}$ = 115 Hz, 2H, m-C_6H_3), 7.83 ($\Delta w_{1/2}$ = 87 Hz, 4H, m-Mes), 2.97 ($\Delta w_{1/2}$ = 41 Hz, 6H, p-CH_3), 1.52 ($\Delta w_{1/2}$ = 150 Hz, 12H, o-CH_3), −0.86 ($\Delta w_{1/2} \approx$ 400 Hz, 1H, p-C_6H_3), 1.92 (s, 12H), 1.85 (m, 4H). UV-vis (THF) [λ_{max}/nm (ε/M^{-1} cm^{-1})]: 379 (2400), 543 (1300), 941 (1000); (toluene): 382 (1700), 509 (800), 788 (900). (CH_2Cl_2): 410 (2500), 491 (1600), 736 (1400), 805sh (1300). Anal. Calc. for $C_{58}H_{66}O_6Cu_2F_6Sb$: C, 57.01, H. 5.44. Found: 56.25; H, 5.63%.

Preparation of $[(ArCO_2)_2Cu_2(THF)_3)]ClO_4$ (3)

To a solution of **1** (0.247 g, 0.268 mmol) in THF (10 mL) was added dropwise a solution of $AgClO_4$ (0.055 g, 0.268 mmol) in THF (3 mL), forming a deep purple solution. The reaction mixture was filtered and concentrated to 5 mL. Addition of pentane (15 mL) and cooling to −20 °C afforded the product as deep purple needle-like crystals (0.089 g, 33%). UV-vis (THF) [λ_{max}/nm (ε/M^{-1} cm^{-1})]: 325 (2700), 367 (2100), 535 (1000), 911 (790); (CH_2Cl_2): 392 (2000), 501 (1200), 753 (1000). Anal. Calc. for $C_{62}H_{74}O_{11}Cu_2Cl$: C, 64.32; H, 6.44. Found: C, 63.40; H, 6.23%.

X-Ray crystal structure determinations

Crystal data, data collection, and refinement parameters for **1** and **3** are listed in Table 2.

A crystal of appropriate size was mounted on a quartz fiber using hydrocarbon oil, transferred to a Siemens SMART diffractometer/CCD area detector, centered in the beam (Mo-Kα; λ = 0.71073 Å; graphite monochromator), and cooled to −100 °C by a liquid-nitrogen low-temperature apparatus. Preliminary orientation matrix and cell constants were determined by collection of 60 10-s frames, followed by spot integration and least-squares refinement. A hemisphere of data was collected using 0.3° ϖ scans. The raw data were integrated (xy spot spread = 1.60°, z spot spread = 0.60°) and the unit cell parameters refined using SAINT.[25] Absorption corrections were applied using SADABS.[26] The data were corrected for Lorentz and polarization effects, but no correction for crystal decay was applied. Structure solutions and refinements were performed (SHELXTL-Plus V5.0[27]) on F^2. All non-hydrogen atoms were refined anisotropically. Hydrogen atoms were placed in idealized positions and refined as riding atoms with relative isotropic displacement parameters.

Table 2 Crystal data, data collection, and refinement parameters for complexes **1** and **3**[a]

	1	**3**
Formula	$C_{58}H_{66}Cu_2O_6$	$C_{62}H_{74}ClCu_2O_{11}$
M	986.19	1157.74
Crystal system	Monoclinic	Orthorhombic
Space group	$P2_1/c$	$Pbcn$
a/Å	8.5214(3)	19.007(1)
b/Å	24.6971(9)	24.185(1)
c/Å	11.8867(4)	25.356(2)
β/°	91.626(1)	90
V/Å^3	2500.6(2)	11656(1)
Z	2	8
D_c/g cm^{-3}	1.310	1.320
μ/mm^{-1}	0.901	0.834
Reflns. measured	11898	67759
Unique reflns. obs.	4343	13335
R_{int}	0.0559	0.0561
Restraints/params.	0/298	40/763
$R1$[b]	0.0639	0.0793
$wR2$[b]	0.1058	0.1587
GOF	1.127	1.173
Largest diff. peak, hole/e Å^{-3}	0.407, −0.354	0.981, −0.730

[a] All structures determined at 173 K, Mo-Kα radiation, refinement based on F^2. [b] For $I > 2\sigma(I)$, $R1 = \Sigma||F_o| - |F_c||/\Sigma|F_o|$, and $wR2 = [\Sigma[w(F_o^2 - F_c^2)^2]/\Sigma[w(F_o^2)^2]]^{1/2}$, where $w = 1/\sigma^2(F_o^2) + (aP)^2 + bP$.

For **3**, the perchlorate anion was found to be disordered over two positions. The first (half occupancy) perchlorate (Cl1, O8, O9, O10, O11) is located near a crystallographic inversion center and is shared between two (inversion) related $[(ArCO_2)_2Cu_2(THF)_3]^+$ units. The second (half occupancy) perchlorate (Cl2, O12, O13, O14, O15) is also located near an inversion center, but it is not coordinated to a metal center. It was necessary to restrain the Cl–O and the "1,3" O–O distances to obtain a reasonable refinement.

CCDC reference numbers 202090 and 202089.

See http://www.rsc.org/suppdata/dt/b3/b301154b/ for crystallographic data in CIF or other electronic format.

Acknowledgements

We thank the NIH (F32-GM19374 to J. R. H. and GM38767 to L. Q.) and the University of Minnesota Undergraduate Research Opportunities and Lando Undergraduate Research Programs (T. I. Z.) for financial support of this research. We also thank Anne M. Reynolds and Victor G. Young, Jr., for assistance with X-ray crystallographic data analysis.

References and notes

1 P. M. H. Kroneck, W. A. Antholine, J. Riester and W. G. Zumft, *FEBS Lett.*, 1988, **242**, 70.
2 M. B. Robin and P. Day, *Adv. Inorg. Chem. Radiochem.*, 1967, **10**, 247.
3 Selected recent references: (*a*) F. Neese, R. Kappl, J. Hüttermann, W. G. Zumft and P. M. H. Kroneck, *J. Biol. Inorg. Chem.*, 1998, **3**, 53; (*b*) M. T. Hay and Y. Lu, *J. Biol. Inorg. Chem.*, 2000, **5**, 699; (*c*) D. W. Randall, D. R. Gamelin, L. B. LaCroix and E. I. Solomon, *J. Biol. Inorg. Chem.*, 2000, **5**, 16; (*d*) S. D. George, M. Metz, R. K. Szilagyi, H. Wang, S. P. Cramer, Y. Lu, W. B. Tolman, B. Hedman, K. O. Hodgson and E. I. Solomon, *J. Am. Chem. Soc.*, 2001, **123**, 5757.
4 (*a*) C. Harding, V. McKee and J. Nelson, *J. Am. Chem. Soc.*, 1991, **113**, 9584; (*b*) M. E. Barr, P. H. Smith, W. Antholine and B. Spencer, *J. Chem. Soc., Chem. Commun.*, 1993, 1649; (*c*) C. Harding, J. Nelson, M. C. R. Symons and J. Wyatt, *J. Chem. Soc., Chem. Commun.*, 1994, 2499; (*d*) J. A. Farrar, V. McKee, A. H. R. Al-Obaidi, J. J. McGarvey, J. Nelson and A. J. Thomson, *Inorg. Chem.*, 1995, **34**, 1302; (*e*) J. A. Farrar, R. Grinter, F. Neese, J. Nelson and A. J. Thomson, *J. Chem. Soc., Dalton Trans.*, 1997, 4083.
5 R. P. Houser, V. G. Young, Jr. and W. B. Tolman, *J. Am. Chem. Soc.*, 1996, **118**, 2101.
6 R. Gupta, Z. H. Zhang, D. Powell, M. P. Hendrich and A. S. Borovik, *Inorg. Chem.*, 2002, **41**, 5100.
7 (*a*) D. D. LeCloux, R. Davydov and S. J. Lippard, *J. Am. Chem. Soc.*, 1998, **120**, 6810; (*b*) D. D. LeCloux, R. Davydov and S. J. Lippard, *Inorg. Chem.*, 1998, **37**, 6814.
8 C. He and S. J. Lippard, *Inorg. Chem.*, 2000, **39**, 5225.
9 S. M.-F. Lo, S. S.-Y. Chui, L.-Y. Shek, Z. Lin, X. X. Zhang, G.-h. Wen and I. D. Williams, *J. Am. Chem. Soc.*, 2000, **122**, 6293.
10 X.-M. Zhang, M.-L. Tong and X.-M. Chen, *Angew. Chem., Int. Ed.*, 2002, **41**, 1029.
11 M. Dunaj-Jurco, G. Ondrejovic, M. Melnik and J. Garaj, *Coord. Chem. Rev.*, 1988, **83**, 1.
12 D. D. LeCloux, A. M. Barrios, T. J. Mizoguchi and S. J. Lippard, *J. Am. Chem. Soc.*, 1998, **120**, 9001.
13 (*a*) L. Que, Jr. and W. B. Tolman, *J. Chem. Soc., Dalton Trans.*, 2002, 653 and references therein; (*b*) D. Lee and S. J. Lippard, *Inorg. Chem.*, 2002, **41**, 827; (*c*) E. Y. Tshuva, D. Lee, W. Bu and S. J. Lippard, *J. Am. Chem. Soc.*, 2002, **124**, 2416.
14 D. Maspoch, D. Ruiz-Molina, K. Wurst, C. Rovira and J. Veciana, *Chem. Commun.*, 2002, 2958.
15 (*a*) M. G. B. Drew, D. A. Edwards and R. Richards, *J. Chem. Soc., Chem. Commun.*, 1973, 124; (*b*) M. G. B. Drew, D. A. Edwards and R. Richards, *J. Chem. Soc., Dalton Trans.*, 1977, 299.
16 D. D. LeCloux and S. J. Lippard, *Inorg. Chem.*, 1997, **36**, 4035.
17 C. Luchinat, A. Soriano, K. Djinovic-Carugo, M. Saraste, B. G. Malmström and I. Bertini, *J. Am. Chem. Soc.*, 1997, **119**, 11023.
18 R. C. Holz, M. L. Alvarez, W. G. Zumft and D. M. Dooley, *Biochemistry*, 1999, **38**, 11164.
19 F. A. Cotton, E. A. Hillard and C. A. Murillo, *J. Am. Chem. Soc.*, 2002, **124**, 5658.
20 A. A. Obaidi, G. Baranovic, J. Coyle, C. G. Coates, J. J. McGarvey, V. McKee and J. Nelson, *Inorg. Chem.*, 1998, **37**, 3567.
21 V. M. Miskowski, S. Franzen, A. P. Shreve, M. R. Ondrias, S. E. W. Williams, M. E. Barr and W. H. Woodruff, *Inorg. Chem.*, 1999, **38**, 2546.
22 L. M. Berreau, J. A. Halfen, V. G. Young, Jr. and W. B. Tolman, *Inorg. Chem.*, 1998, **37**, 1091.
23 (*a*) G. J. Kubas, *Inorg. Synth.*, 1979, **19**, 90; (*b*) G. J. Kubas, *Inorg. Synth.*, 1990, **28**, 68.
24 (*a*) J. R. Hagadorn, L. Que, Jr. and W. B. Tolman, *J. Am. Chem. Soc.*, 1998, **120**, 13531; (*b*) J. R. Hagadorn, L. Que, Jr. and W. B. Tolman, *Inorg. Chem.*, 2000, **39**, 6086.
25 SAINT, Bruker Analytical X-ray Systems, Madison, WI, 1999.
26 SADABS: An empirical correction for absorption anisotropy, R. Blessing, *Acta Crystallogr., Sect. A*, 1995, **51**, 33.
27 G. M. Sheldrick, SHELXTL-Plus V5.0, Program for refinement of crystal structures, University of Göttingen, Germany, 1997.